



Research article

Different particle sizes of *Momordica charantia* leaf powder modify the rheological and textural properties of corn starch-based 3D food printing ink

Meiqi Fan^a, Young-Jin Choi^{b,c}, Nishala Erandi Wedamulla^{b,c,d}, Seok-Hee Kim^{b,c}, Sung Mun Bae^e, DaEun Yang^f, Hyo Kang^f, Yujiao Tang^g, Sang-Ho Moon^a, Eun-Kyung Kim^{h,i,*}

^a Division of Food Bioscience, College of Biomedical and Health Sciences, Konkuk University, Chungju, 27478, Republic of Korea

^b Department of Food Science and Nutrition, College of Health Science, Dong-A University, Busan, 49315, Republic of Korea

^c Department of Health Sciences, The Graduate School of Dong-A University, Busan, 49315, Republic of Korea

^d Department of Food Science and Technology, Uva Wellassa University, Badulla, 90000, Sri Lanka

^e Gyeongnam Agricultural Research and Extension Services, Jinju, 52733, Republic of Korea

^f BK-21 Four Graduate Program, Department of Chemical Engineering, Dong-A University, Busan, 49315, Republic of Korea

^g School of Bio-Science and Food Engineering, Changchun University of Science and Technology, Changchun, 130600, China

^h Nutritional Education Major, Graduate School of Education, Dong-A University, Busan, 49315, Republic of Korea

ⁱ Nutrionics Lab. Co., Ltd., Busan, 49315, Republic of Korea

ARTICLE INFO

Keywords:

M. charantia leaf powder
Particle size
Starch
3D printing
Food ink

ABSTRACT

The study determined the effect of incorporating *Momordica charantia* leaf powder (MCLP) into corn-starch 3D food-printing ink as a functional ingredient. The effects of the particle size (75, 131, and 200 μm) and quantity of MCLP on 3D printing performance, structural, textural, and rheological properties of corn starch gel were evaluated with different concentrations (5, 10, and 15 % (w/w)) of corn starch. The viscoelastic properties of food inks were determined considering their behavior during extrusion and self-recovery after printing. Scanning electron microscope was used to characterize the microstructure. Based on the results, a high starch content (15 %) with 5 % MCLP was more favorable for 3D food printing. In addition, 3D printing performance, textural and rheological properties of formulated ink was mainly governed by the particle size of MCLP. The food ink with a 5 % mass fraction of 200 μm MCLP had the highest printing precision and the best masticatory properties.

1. Introduction

Momordica charantia (*M. charantia*), which belongs to the Cucurbitaceae family, is a tendril-climbing annual plant commonly known as bitter melon/gourd. *M. charantia* leaves (MCLs) have been used in folk medicine to treat various ailments, including diabetes, obesity, and inflammation [1]. A water extract rich in cucurbitane-type triterpenoids was found to reduce the body weight and energy

* Corresponding author. Nutritional Education Major, Graduate School of Education, Dong-A University, Busan, 49315, Republic of Korea.

E-mail addresses: fanmeiqi@kku.ac.kr (M. Fan), choiyoung11@donga.ac.kr (Y.-J. Choi), 2178445@donga.ac.kr (N.E. Wedamulla), 2371906@donga.ac.kr (S.-H. Kim), smbae@korea.kr (S.M. Bae), 1830133@donga.ac.kr (D. Yang), hkang@dau.ac.kr (H. Kang), yuanxi00@126.com (Y. Tang), moon0204@kku.ac.kr (S.-H. Moon), ekkimkr@dau.ac.kr (E.-K. Kim).

<https://doi.org/10.1016/j.heliyon.2024.e24915>

Received 7 September 2023; Received in revised form 12 January 2024; Accepted 17 January 2024

Available online 1 February 2024

2405-8440/© 2024 The Authors. Published by Elsevier Ltd. This is an open access article under the CC BY-NC-ND license (<http://creativecommons.org/licenses/by-nc-nd/4.0/>).

Abbreviations

MCLP	Momordica charantia leaf powder
IDDSI	International Dysphagia Diet Standardization Initiative
MCL	M. charantia leaves
SEM	Scanning electron microscopy

intake of high-fat diet-fed mice and inhibit adipogenesis in 3T3-L1 pre-adipocytes [2]. Moreover, momordicine I, II, and IV and 3 β ,7 β , 25-trihydroxycucurbita-5,23(E)-dien-19-al isolated from MCL were demonstrated to reduce periodontal pathogen- or Cutibacterium acne-induced inflammatory responses in humans [3]. MCL is used to treat various skin and stomach ailments owing to its antimicrobial properties. *M. charantia* also functions as an antimicrobial agent [4]. Tea and juice prepared from MCL are popular preparations. MCL is also consumed as a vegetable; however, as chewing is required, it is not suitable for people with chewing or swallowing difficulties.

3D printing is the process of creating three-dimensional objects by positioning layers of material on top of each other. 3D food printing enables the innovative development of novel and personalized food products and the expansion of food supply channels. Owing to these characteristics, 3D food printing has been extensively used in functional food development. Recently, 3D food printing research related to dysphagia has been growing rapidly owing to the identification of an increasingly aging population as one of the major global issues. Dysphagia is characterized by difficulties in swallowing, which leads to abnormal delays in food bolus movement [5]. Currently, most vegetable-based foods for elderly people are pureed or mashed to make them less palatable and appetizing. 3D food printing has identified as one of the promising techniques that formulates more appealing foods with required textural modifications for dysphagia. Furthermore, 3D food printing has gained popularity in texture-modified diets owing to its' ability to formulate food inks with different textural properties and these texture-modified diets are basic requirement for dysphagia [6]. Thus, the use of MCL as a raw material and the utilization of its physical and nutritional properties to adapt food formulations can meet consumer demands for personalized nutrition owing to its promising health characteristics.

The keys to the successful development of 3D food printing are printing materials and the accuracy and efficiency of the process [7]. For the 3D food printing process, the material must have sufficient fluidity to allow continuous and uniform extrusion and should retain the product shape after extrusion. Studies on natural polymer hydrogels have revealed their ease of use as they usually exhibit non-Newtonian fluid behavior [8]. Currently, the availability of 3D edible gel printing materials is limited. The rheological properties of foods can be improved by optimizing food formulations to ensure easy extrusion of materials and minimal deformation after printing. The rheological and textural properties of 3D food printing inks depend mainly on the ingredients. Therefore, the incorporation of functional materials into 3D food-printing ink significantly alters the material characteristics of the ink, especially when incorporated in the powder form. This change is largely affected by the particle size of the incorporated material [9]. Therefore, it is worth to investigate the structural and rheological modifications of MCLP incorporated corn starch gel as different particle sizes significantly alter the 3D food printing performance and these findings are vital for the formulation of functionals ingredients incorporated 3D food printing ink.

Food processing uses corn starch as a thickener, water-holding agent, and binder to enhance the gel properties, water-holding capacity, and elasticity of foods [10]. The 3D printability of MCL can be enhanced by the addition of corn starch. The amount of corn starch added to the MCL 3D printing ink and the particle size of the MCL powder (MCLP) can influence the apparent viscosity, rheological properties (ease of migration), print results (appearance, shape, and set), and gel characteristics. However, few studies have explored the modification of 3D food printing ink with the addition of functional ingredients, especially with functional powders of different particle sizes. Bridging this research gap is thus vital for the remarkable growth of functional ingredients added customized 3D food printing ink. Owing to this urgent need, the aim of the current study was to determine the effect of different MCL particle sizes on the rheological and textural characteristics of corn-starch 3D food-printing gel as a functional ingredient. This study investigated the gel strength, texture, rheological properties, and 3D printing performance of MCLP 3D printing ink with different quantities of corn starch and determined the optimal amount of corn starch and particle size of MCLP for 3D food printing. Further, the current study hypothesizes that the particle size and content of MCLP govern the textural, rheological and 3D printing performance of MCLP-added corn starch ink. Collectively, this study provides a theoretical basis for the application of MCLP in the development of functional inks for 3D food printing.

2. Materials and methods

2.1. Materials

Corn starch (amylose content 29.60 ± 0.68 %) was purchased from Ttuleban (Gyeonggi-do, South Korea). Fresh MCL was purchased from a local supermarket (Shandong, China). The separated samples were washed under running tap water, dried by natural withering for two weeks, powdered, and placed in a desiccator for further use. The moisture, ash, crude protein, crude lipid and crude fiber contents of the MCLP were recorded as 15 ± 0.50 , 17.93 ± 0.47 , 10.25 ± 0.51 , 3.03 ± 0.76 , 25.31 ± 0.32 % (DW) [11]. Dry sieving of the MCLP particles was performed using an orbital shaker (SH30 Orbital Shaker, Fine PCR, Korea). Particle sizes of 75, 131, or 200 μm were obtained using stainless-steel sieves with pore sizes of 45, 106, 150, 212, and 250 μm ; these three particle sizes represented different samples in the following study. The average particle size of the corn starch used in the study was 131 μm .

2.2. Food ink mixture preparation

Deionized water was used to prepare aqueous solutions of the MCLP and starch blends. Formulations consisting of MCLP and starch 20 % (w/w) were used to determine whether the particle size significantly influenced the rheological properties and printing performance. First, corn starch was prepared as a starch suspension at concentrations of 15 %, 10 %, and 5 % (w/v, dry basis). The starch suspension was gelatinized via heating to 90 °C and manually stirred 3 times at 5-min intervals. After cooling to 60 °C, the MCLP of various particle sizes were incorporated in the starch suspensions (5 %, 10 %, and 15 %) and stirred for 30 min until a homogeneous food ink formulation was obtained. Nine different inks were tested, and their compositions are listed in [Supplementary Table 1](#). During the preparation, the container was covered with a thin plastic wrap to prevent moisture evaporation. A total reaction volume of 100 mL was used. Immediately after the material was cooled, it was filled in a syringe and placed at 4 °C overnight (12 h) for the formation of the starch gel for 3D printing.

2.2.1. Scanning electron microscopy (SEM)

Field-emission scanning electron microscopy (SCIOS 2; Thermo Fisher Scientific, Hillsboro, OR, USA) was used to determine the microstructure of the food inks at an accelerated voltage of 2 kV and a working distance of 7 mm. Each food ink mixture was coated with gold (10 mA for 120 s) under vacuum using a sputter coater (Cressington 108 Auto Sputter Coater; Cressington Scientific Instruments). A magnification of $\times 250$ was used for MCLP and $\times 500$ was used for the ink mixtures.

2.3. Water holding capacity (WHC)

Chen and coworkers described a modified method for determining the WHC of MCLP samples of different sizes. First, empty centrifuge tubes (W1) were weighed, and 0.05 g of each MCLP (W2) was added to each tube containing 1 mL of deionized water. The tubes were placed in a water bath for 1 h at 60 °C and then transferred to cold water for 30 min. The samples were centrifuged for 20 min at 10,000 rpm in a refrigerated centrifuge. After removing the supernatant, the tubes containing the residue (W3) were weighed [12]. The following formula was used to calculate the WHC: $\text{WHC (g/g)} = (\text{W3} - \text{W1} - \text{W2}) / \text{W2}$.

2.4. Dynamic viscoelastic properties of 3D printing food inks

Dynamic viscoelasticity and viscosity of the food inks were measured using a rheometer (Discovery HR-3; TA Instruments, New Castle, DE, USA) with a parallel plate of 20 mm diameter and a gap of 1 mm. The dynamic viscoelastic properties were measured in the range of 0.1–100 rad/s, and viscosity parameters were determined in the shear rate range of 0.1–100/s. The experimental measurements were conducted at 25 °C, and the gel was equilibrated at room temperature (25 °C) for 7 min prior to each measurement.

2.5. Texture properties of 3D printing food inks

A texture analyzer (Brookfield CT3 Texture Analyzer; Brookfield Engineering Laboratories, Middleboro, MA, USA) was used to assess the textural properties of food inks with different formulations, according to a previously described method. Each food ink was placed in a cylindrical plastic container (35 mm in diameter and 20 mm in height) positioned at the center of the platform. The force-time curves were measured using a 13 mm-diameter cylinder probe. Height and weight calibrations were performed prior to testing. There were two compression cycles: both tests were conducted at 10 mm/s and the post-test was conducted at 1 mm/s. The holding time was 0 s and the trigger force was 7 g. The tests were conducted in triplicate at room temperature (25 °C).

2.6. Printability assessment of 3D printing food inks

An extrusion 3D printing system (Choco J; LSB Co., Ltd., South Korea) was used for the printability experiments. In this study, a hollow cylinder with dimensions of 20 mm \times 20 mm was designed using the 3D modeling software Tinkercad (Autodesk, Inc., San Rafael, California, USA). The objects were sliced using the open-source 3D slicer software, Ultimaker Cura (version 4.12.1). The printing conditions were set as follows: nozzle diameter, 1 mm; layer height, 0.8 mm; nozzle moving speed, 5 mm/s; and extruder moving speed, 100 mm/s. A temperature of 25 ± 1 °C was used for all printing experiments.

The printing accuracy was calculated using the following equation:

$$\text{Printing accuracy (\%)} = ((1 - (D_{TI} - D_{IS}) / D_{IS}) + (1 - (D_{TO} - D_{OS}) / D_{OS}) + (1 - H / H_S) + (1 - (D_{BI} - D_{IS}) / D_{IS}) + (1 - (D_{BO} - D_{OS}) / D_{OS})) / 5 \times 100$$

where D_{TI} is the top inner diameter (mm), D_{IS} is the set inner diameter of the model (mm), D_{TO} refers to the top outer diameter (mm), D_{OS} is the outer diameter of the model (mm), H denotes the height of the 3D-printed product (mm), where H_S represents the set height of the model (mm), D_{BI} refers to the inner diameter of the bottom (mm), and D_{BO} refers to the outer diameter of the bottom (mm).

2.7. FTIR spectrum of 3D printing food inks

Infrared spectra were obtained using a Nicolet iS50 FTIR spectrometer (Thermo Fisher Scientific, Waltham, MA, USA) equipped with a KBr/Ge beam splitter, deuterated triglycine sulfate detector, and smart iTX-iD7 attenuated total reflectance sampling accessory

with a diamond crystal. The FTIR spectra were collected from 400 cm^{-1} – 4000 cm^{-1} . Each ink mixture was scanned 16 times at a resolution of 8 cm^{-1} . The spectra were normalized and corrected for baseline effects using OMNIC spectra software (version 8.0; Thermo Fisher Scientific).

2.8. Syneresis of 3D printing food inks

A protocol adapted from the filter paper blotting method was used to analyze the syneresis of the hydrogel [13]. Food inks of different formulations were placed on Whatman Grade 4 filter paper with a radius of 1.25 cm at the center of the experiment. Food inks were flattened to cover a circle of 1 cm in diameter. After 30 min of fluid spreading on the filter paper, the samples were photographed. To identify the contours of the water ring, the area covered by the fluid was measured and analyzed using ImageJ software. A ruler was used as a reference for image analysis and photographed with the filter paper.

2.9. International dysphagia diet standardization initiative (IDDSI) test of 3D food inks

A fork pressure test was conducted on 3D printed cuboids (15 mm edge length), during which thumb pressure was applied to the surface of the food ink to observe its deformation [5]. Of note, blanching occurs when the pressure is greater than the mean arterial blood pressure (approximately 17 kPa), which is similar to tongue pressure during swallowing. The samples must be compressed with the fork pressure categorized according to the IDDSI framework and should not regain their original shape after pressure release. The spoon-tilt test was performed by scooping a teaspoon of food ink, holding the spoon steadily above a plate, and slowly tilting the spoon sideways. The behavior of the food ink on the spoon during tilting was compared with the IDDSI descriptions. In accordance with the IDDSI, a level 5 minced and moist dysphagia diet must demonstrate the following characteristics: can be eaten with a fork, spoon, or chopsticks, depending on the individual's mastery of hand control; can be easily scooped and shaped on a plate; have small lumps visible within the food; and can be easily squashed.

2.10. Statistical analysis

Origin 8.0 software (Stat-Ease Company, Minneapolis, MN, USA) and GraphPad Prism (version 8.4; GraphPad Software, San Diego, CA, USA) for Tukey's test ($p < 0.05$) were used to prepare graphs and determine the statistical significance, respectively.

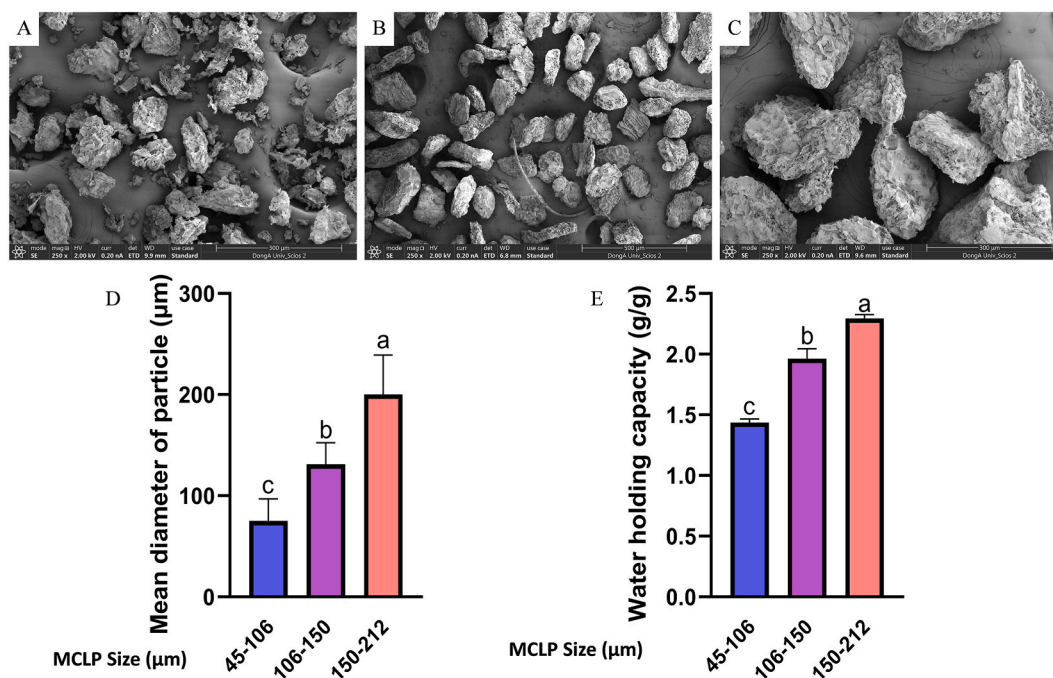


Fig. 1. Morphological and physico-chemical characteristics of MCLP. SEM images of (A) 45–106 μm, (B) 106–150 μm, and (C) 150–212 μm particle sizes of MCLP. (D) Mean diameter (μm) and (E) Water holding capacity (g/g) of MCL particle.

3. Results and discussion

3.1. Morphological analysis and WHC of MCLP

The morphological characteristics of the MCLP particles are shown in Fig. 1. MCLP with a particle size of 200 μm displayed

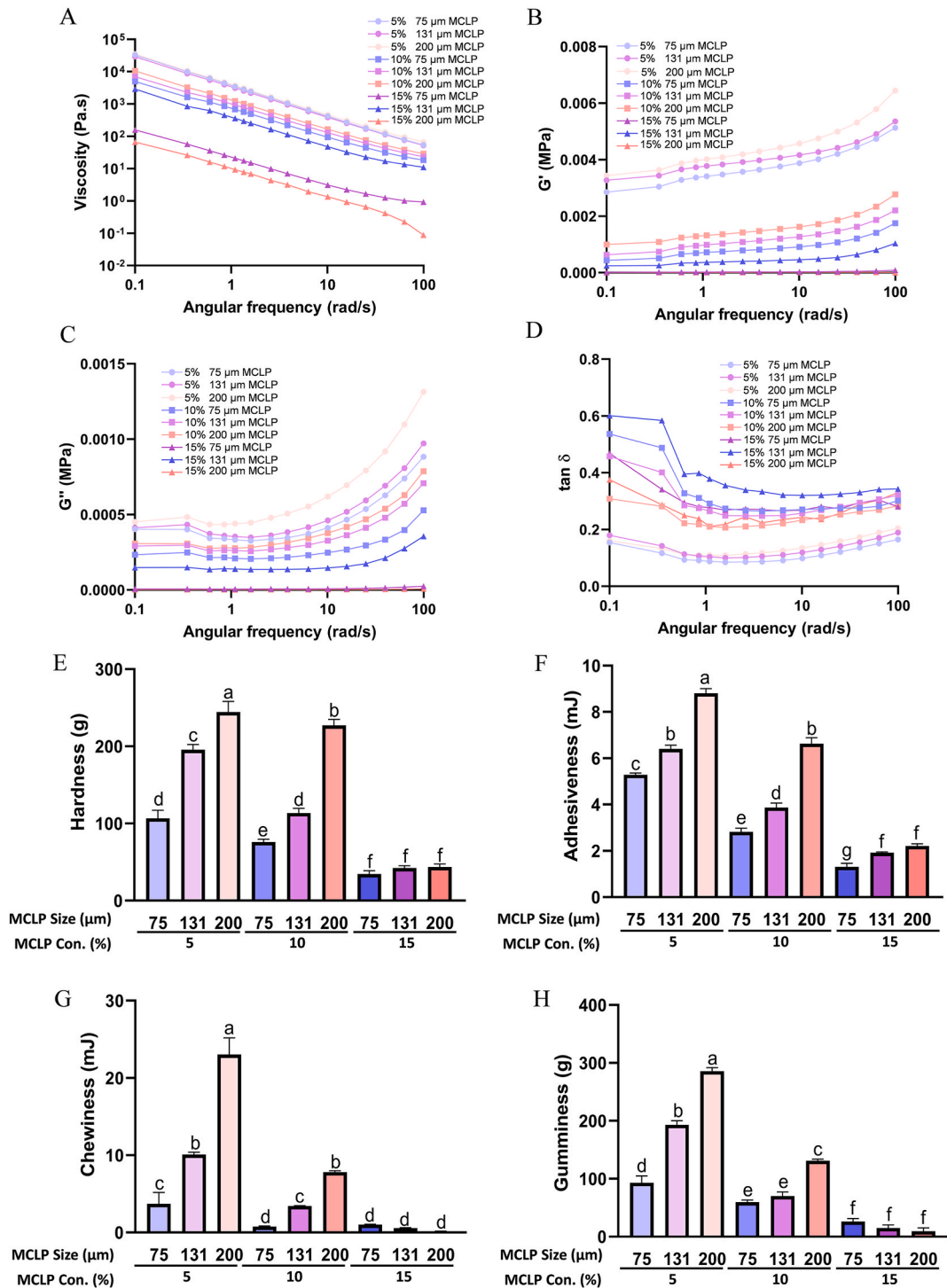


Fig. 2. Rheological behavior and textural properties of MCLP-added corn starch inks. (A) Viscosity, (B) G' , (C) G'' , and (D) $\tan \delta$ (E) Hardness, (F) Adhesiveness, (G) Chewiness, and (H) Gumminess of MCLP-added corn starch ink.

irregular polygonal morphology with random pores and a rough cellular structure. This result might be due to MCL being rich in fibers, which are not crushed during milling owing to their robust and hard tissue structure. They may have originated from petioles, midribs, or veins [14]. Irregular and compact particles with sharp edges and remarkable indentations due to milling were observed in MCLP with particle sizes of 131 μm and 75 μm ; these particles were efficiently packed with minimal space between them. Smaller particles may originate from the delicate structure of the thin layers and small reticulate veins, which can easily be crushed into fine particles [15]. The MCLP particle size of 200 μm had a more porous structure on the surface than the smaller particle size, which is attributed to the different rheological and textural properties of MCLP-added corn starch gel. Moreover, a previous study reported that fiber content increased with the increasing particle size [16]. Consequently, high fiber content of 200 μm particle size of MCL powder may be contributed to exhibit deviations in 3D printing performance.

According to Raghavendra and coworkers, the water-holding capacity of a powder refers to the amount of water that it can hold under atmospheric pressure and gravity [17]. The WHC of the MCLP increased significantly as the particle size increased. Powder properties, including porosity, surface area, bulk density, and ingredient composition, may differ due to grinding and sieving. Generally, the WHC is related to the microstructure of vegetable powders, their bulk density, and their water-binding sites [9]. Based on the results of the current study, particle diameter and WHC exhibited a positive relationship, which may be attributed to the porous structure and surface characteristics of the particle size, where more pore structures with larger particle sizes contributed to a high WHC.

3.2. Rheological characteristics of 3D printing food inks

As shown in Fig. 2A, the viscosity of food ink increases with increasing angular frequency, resulting in shear thinning and non-Newtonian pseudoplastic fluid behavior [18]. Accordingly, apparent viscosity increased as the starch content increased. A higher apparent viscosity results in higher bond strength during layer deposition [19]. Fig. 2B–D shows the plots of storage modulus (G'), loss modulus (G''), and $\tan \delta$ versus angular frequency (ω) for MCLP mixtures of different particle sizes. In Fig. 2B and C, both G' and G'' of the MCLP ink mixtures increased with starch addition and an increase in particle size, indicating that they could provide a degree of rigidity to the MCLP ink mixtures. G' was higher than G'' in all inks, and G' and G'' increased as the angular frequency increased, indicating weak gel characteristics [20]. The increase in G' and G'' values with increasing particle size may be related to the microstructure and bulk density of the particles. Larger particles with high porosity exhibited a low bulk density and a relatively high bulk size when MCLP was incorporated at the same mass ratio. Variations in the bulk size of the dispersion system may have a significant effect on printability and printing performance. Moreover, high fiber content of larger particle size also equally contributed to exhibited rheological properties. Studies have reported that crude fiber alters the flow properties increasing the rigidity of the material [21]. Accordingly, MCLP and corn starch blend formulated with larger particle size showed higher G' and G'' attributed to high fiber content. The $\tan \delta$ of all groups decreased as the angular frequency increased, and the overall trend was generally similar. In addition, the $\tan \delta$ values for all groups were less than 1, indicating elastic behavior in all inks. Thus, the inks exhibited a solid nature and could self-retain their 3D printed structures after printing [22]. As shown in Fig. 2D, the $\tan \delta$ value of the group with 15 % starch was lower than that of the other groups, indicating that the 15 % starch-inks tended to be more solid than the other inks, indicating better elasticity, stability, and shape-retention properties of inks with increasing starch content and particle size, which aligns with the printed products.

The relationship between the WHC and rheological properties is well documented [23]. Our results proved the positive correlation between particle size and WHC (Fig. 1), ultimately demonstrating the potential relationship between particle size, WHC, and rheological properties. Thus, particle size markedly affects the correlation between the WHC and rheological properties of ink formulations.

3.3. Textural properties of 3D printing food inks

The effects of starch content and particle size on the textural properties of food ink are shown in Fig. 2. As particle size increased, hardness, adhesiveness, chewiness, and gumminess of the ink significantly increased (Fig. 2E–H), aligning with the rheological parameters. This increase was more significant with a high starch content, indicating that an increase in starch is beneficial for the printing and molding processes [24], where MCL and corn starch blend perfectly to form a gel with excellent textural properties. The qualitative properties of MCLP ink have a substantial impact on the efficiency of 3D printing. When the hardness and adhesiveness of the ink are extremely low, its ability to counteract the potential energy loss is reduced, which affects the extrusion of the ink and reduces its printability [25]. The higher the mastication of the slurry during helical extrusion of the ink by the printer, the lower the probability of breaking into strips during extrusion. Moreover, a certain amount of gumminess facilitates ink formation [26]. The increase in the hardness and adhesiveness of the ink facilitated by increasing starch concentration is attributed to the swelling of starch macroparticles filling the porous structure, resulting in increased extrusion pressure between the macromolecules and a more stable gel structure [27]. Conversely, a decrease in the concentration of tapioca starch decreased the concentration of macromolecules in the ink, thereby reducing cross-linking and the formation of straight-chain links in starch, resulting in the formation of a more brittle gel ink with less hardness and elasticity [28]. This result is consistent with that of the current study, in which the hardness of all inks decreased at the lowest concentration (5 %) of corn starch, regardless of particle size. Thus, at low starch concentrations, particle size is a less significant factor governing textural properties, whereas at high concentrations, particle size plays a central role in governing the textural properties. Further, at higher MCLP contents, ink formulations contained high amounts of fiber compared to ink formulations with low content of MCLP. Therefore, water absorption of fiber is more prominent with high MCLP content, and this may lead to low hardness by reducing the degree of cross-linking [21]. However, hardness increased with the increase in particle size. This may be

attributed to strong particle-particle interactions at larger particle size of MCLP. Previous study also reported similar results where hardness increased with increase in particle size of spinach powder [9].

3.4. Printing performance of MCLP-added corn starch inks

A hollow cylinder was printed to assess the 3D printability of different ink formulations. Fig. 3 shows a photograph of the products printed using the MCLP ink mixtures. As shown in Fig. 3A, some differences in the surface properties and overall particle size were observed among the inks with different particle sizes and starch contents. The samples printed using 10 % MCLP ink were stacked during printing but collapsed in shape owing to poor structural stability. This result is because lower hardness and gumminess of 10 % MCLP ink ensured smooth extrusion, but its lower G' and G'' resulted in insufficient mechanical strength to maintain stable printed structure. Further, all 15 % MCLP inks failed to print the target objects may be attributed to increased rigidity of the gel due to high fiber content. All 5 % MCLP inks were printed smoothly, regardless of the particle size. Despite being structurally stable, the 75 and 131 μm MCLP inks displayed a rougher surface with many small holes in the printed samples owing to broken strips. This result was due to poor extrusion of the material and the tendency of the strips to break despite the sufficient structural stability of the printed samples. These findings are consistent with the previous textural and rheological results. In contrast, 5 % 200 μm MCLP ink displayed more structural stability owing to higher fiber content. High fiber content results in increased rigidity of printing material while maintaining the shape of printed structure resulting in less deformed printed object [20]. Fig. 4B shows some models successfully printed using the 5 % 200 μm MCLP ink, demonstrating that the 5 % 200 μm MCLP ink allows accurate 3D printing with sufficient mechanical strength to maintain the structural stability.

Fig. 3C–J summarizes the 3D printing performance of MCLP-added corn starch gel. The collapse of the printed products decreased

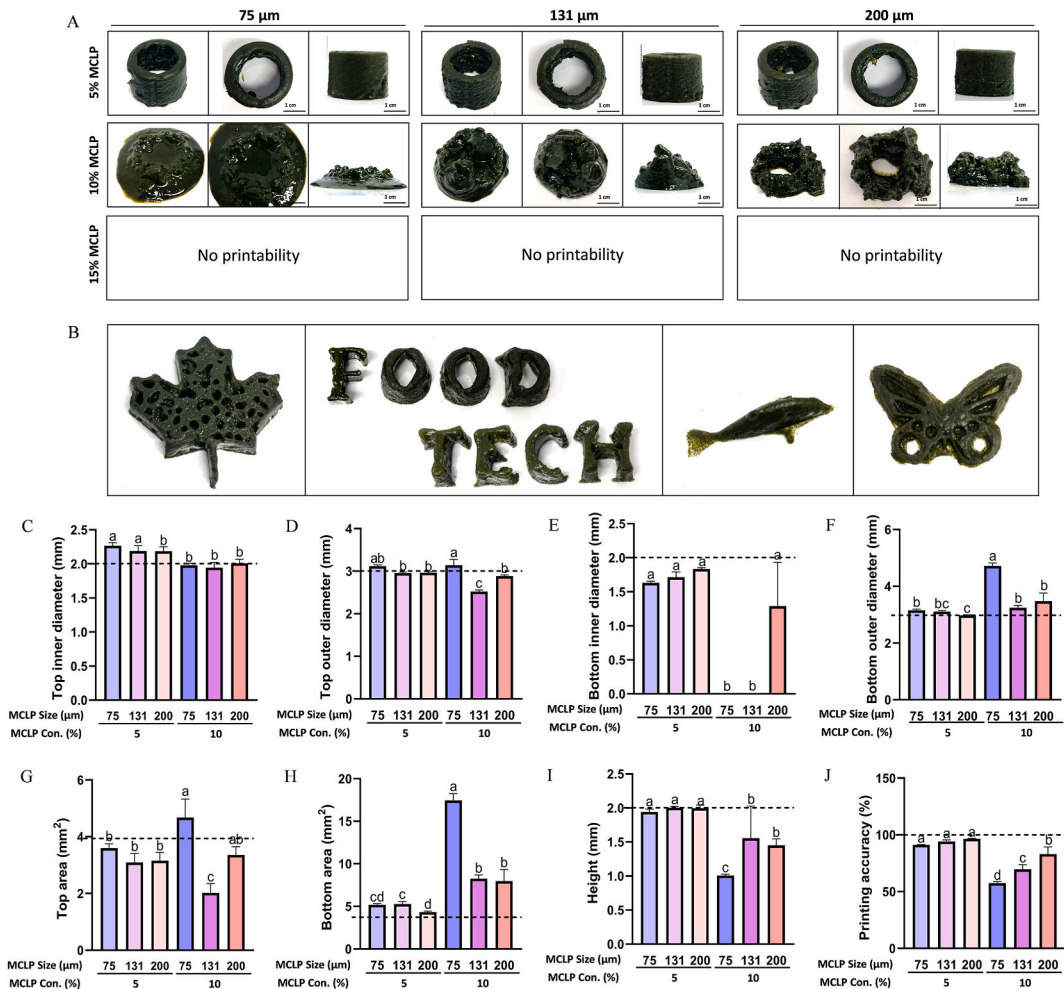


Fig. 3. Effect of different particle sizes of MCLP on 3D printing performance of corn starch ink (A) 3D models printed with different formulations of MCLP and corn starch, (B) Images of different 3D models printed with 5 % 200 μm ink. Dimensions of 3D model printed with different MCLP and corn starch formulations: Top inner (C) and outer (D) diameter; Bottom inner (E) and outer (F) diameter; (G) Top area; (H) Bottom area; (I) Height; (J) Printing accuracy.

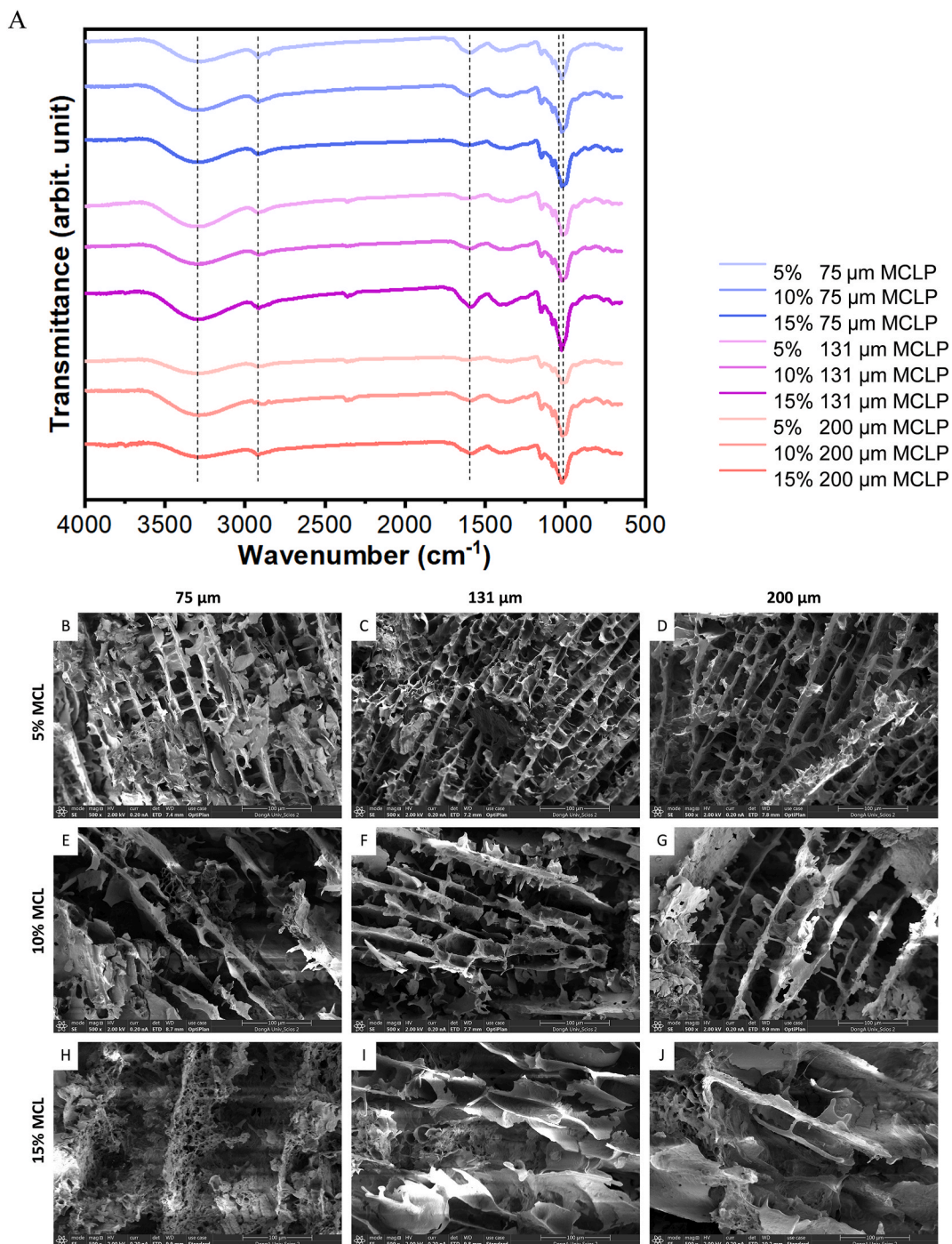


Fig. 4. (A) FTIR spectra of the MCLP-added corn starch ink. Microstructure of the different ink formulations. (B) 5 % 75 μm MCLP, (C) 5 % 131 μm MCLP, (D) 5 % 200 μm MCLP, (E) 10 % 75 μm MCLP, (F) 10 % 131 μm MCLP, (G) 10 % 200 μm MCLP, (H) 15 % 75 μm MCLP, (I) 15 % 131 μm MCLP, and (J) 15 % 200 μm MCLP.

as the size of the MCLP particles increased, indicating that the MCLP large particles improved the support of the starch gel samples. As shown in Fig. 3C–I, as the MCLP particle size increased, the top diameter and bottom area of the printed product gradually decreased while the height increased, which was more consistent with the model setup. Notably, the material is stacked layer by layer during 3D printing, producing samples without sagging and collapsing as the most critical criteria for effective printing [29]. As shown in Fig. 3I, the height of the prints gradually increased as the size of the MCLP particles increased, with 5 % 200 μm MCLP reaching a height of 19.7 mm. The inclusion of large MCLP particles could alleviate the degree of sagging and collapse of the starch gel to some extent.

Similarly, the printing accuracy of the prints tended to increase as the MCLP particle size increased (Fig. 3J).

The particle size of MCLP markedly affected the printing performance at a lower concentration than at a high concentration of corn starch. Similarly, the top outer diameter, bottom inner diameter, top area, and height did not exhibit significant differences among the different particle sizes at a corn starch concentration of 15 %. However, the top outer diameter, bottom inner diameter, top area, bottom area, and height significantly differed between the different particle sizes at a corn starch concentration of 10 %, and a higher particle size induced better printing characteristics. A similar trend was observed for printing accuracy, where the largest particle size exhibited a higher printing accuracy at 10 % corn starch concentration. In contrast, the 15 % corn starch-added gel displayed the highest printing accuracy among all gel formulations, regardless of particle size. Therefore, at higher concentrations of corn starch, the particle size of the incorporated powder is less significant at improving the 3D printing performance, while at low concentrations of corn starch, the particle size of the incorporated powder plays a central role in improving the 3D printing performance. Thus, our findings suggest that both the particle size and amount of incorporated powder play a pivotal role in improving the printing performance of 3D printing gels. Further, according to the results of the current study low MCLP content (5 %) showed better printing performance. Similarly, the amount of powder incorporated into the 3D food-printing gel is governed by the particle size of the powder.

3.5. FT-IR absorption characteristics of 3D printing food inks

Fig. 4 shows the typical shared peaks in the FT-IR spectra of 3D printing inks with different particle sizes and starch contents. The

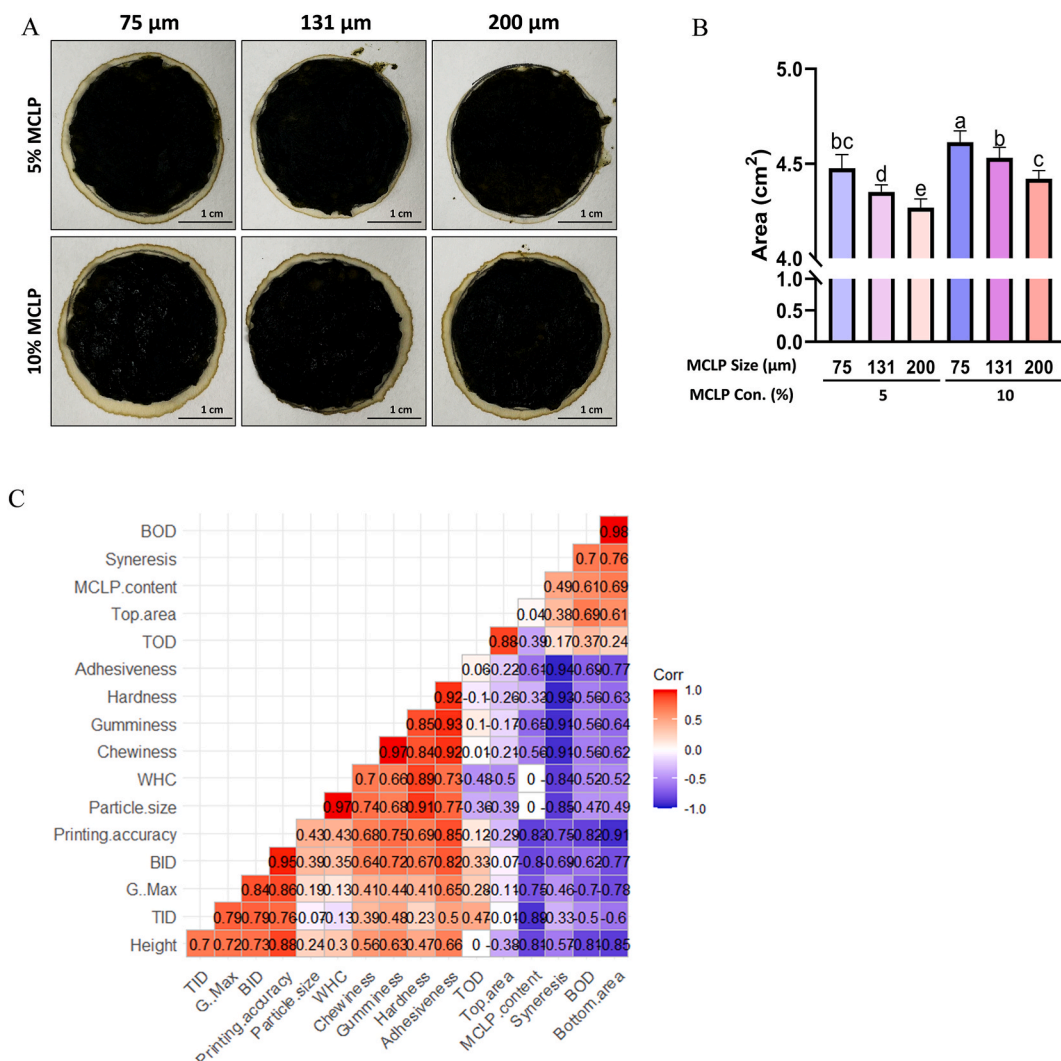
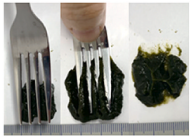





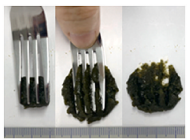







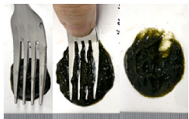





Fig. 5. Syneresis and correlation matrix of MCLP-added corn starch ink. (A) Syneresis measurement. (B) Spreading of food inks measured in area covered by the liquid leaking from food inks on the filter paper. (C) Heatmap of the distribution of correlation coefficients between the particle size, gel properties, and printing performance of the printed products.

Table 1
Classification of samples based on the IDDSI test.

Sample	Fork pressure test	Fork drip test	Spoon tilt test	Comments
5 % 75 μm MCLP		 Description: Ink sits in a pile above the fork. Does not drip continuously through a fork.	 Description: Holds its shape on a spoon. Fails off hardly if the spoon is tilted. Sticky.	Level 5- Minced and moist
5 % 131 μm MCLP		 Description: Ink sits in a pile above the fork. Does not drip continuously through a fork.	 Description: Holds its shape on a spoon. Fails off hardly if the spoon is tilted. Sticky.	Level 5- Minced and moist
5 % 200 μm MCLP		 Description: Ink sits in a pile above the fork. Does not drip continuously through a fork.	 Description: Holds its shape on a spoon. Fails off hardly if the spoon is tilted. Sticky.	Level 5- Minced and moist
10 % 75 μm MCLP		 Description: Drips slowly in dollops through the prongs of a fork.	 Description: Hard holds its shape on a spoon. Fails off easily if the spoon is tilted. Not firm.	Not classified

(continued on next page)

Table 1 (continued)

Sample	Fork pressure test	Fork drip test	Spoon tilt test	Comments
10 % 131 μm MCLP	 Description: Push down on piece with fork ink squash completely and not regain its shape.	 Description: Ink sits in a pile above the fork. Does not drip continuously through a fork.	 Description: Hard holds its shape on a spoon. Fails off if the spoon is tilted. Not firm. Sticky.	Level 4- Pureed
10 % 200 μm MCLP	 Description: Push down on piece with fork ink squash completely and not regain its shape.	 Description: Ink sits in a pile above the fork. Does not drip continuously through a fork.	 Description: Hard holds its shape on a spoon. Fails off if the spoon is tilted. Not firm. Sticky.	Level 4- Pureed

intensity of the absorption peaks is expressed in terms of transmittance. The higher the transmittance, the weaker the absorption intensity. The broad peak near 3310 cm^{-1} corresponded to the stretching vibration peak of the hydroxyl group in starch, the absorption peak at 2930 cm^{-1} represented the $-\text{CH}$ stretching vibration peak of starch, and the peak at 1625 cm^{-1} represented the characteristic $-\text{OH}$ absorption peak of starch, which is common in starch-like substances [30,31]. When small molecules are incorporated into the single-helix cavity of straight-chain starch through hydrophobic interactions, an inclusive crystalline complex is formed, and the characteristic IR absorption peaks are shielded to some extent [32]. As shown in Fig. 4, typical infrared characteristic absorption peaks of starch are present in the spectrum, but the major MCL characteristic absorption peaks are absent. Furthermore, no complementary absorption peaks appeared in the treated 3D printing inks with increasing MCLP content, indicating that no new functional groups were generated by the addition of MCLP to starch. Such findings indicate the absence of new substances and the emergence of safety issues after the treatment of 3D printing inks via multiple strategies. Moreover, the addition of MCLP did not significantly affect starch gelatinization as no marked differences were observed in the peaks at 1022, 1047, and 995 nm. Accordingly, the absorbance ratios at $1047/1022$ and $1022/995\text{ cm}^{-1}$ were not markedly different among the corn-starch gels prepared with different MCLP particle sizes and contents (Fig. 4A), which represents the short-range molecular order of the starch [33]. Our studies revealed that the incorporation of MCLP into pre-gelatinized corn starch did not lead to the formation of any chemical bonds, and the observed changes in rheological, textural, and printing characteristics were solely attributed to the physical binding of starch and the porous surfaces of MCLP. As a result, the functional properties of the MCL remained intact after formulation into the 3D printing gel and delivered the expected functional properties.

3.6. Scanning electron microscopy (SEM) of 3D printing food inks

Fig. 4B–J shows the microstructures of the MCLP ink mixtures. The ink with 5 % MCLP exhibited a reticulate structure, uniform distribution of pores, and thinner pore walls. This result may be due to the small number of MCLP molecules adhering to the surface of the dextrinized starch molecules, which acted as a bridging agent and strengthened the network of dextrinized starch molecules [34]. The ink with 10 % MCLP exhibited a cross-linked porous structure; however, the pore sizes were not uniformly distributed, and the pore walls were thicker, which might be due to the surface of the starch molecules being covered by MCLP, resulting in the formation of a rigid structure [35]. This phenomenon explains the rough and grainy surfaces of the samples printed using the 10 % MCLP ink. The ink with 15 % MCLP did not form a continuous mesh structure and exhibited a lamellar powdery surface. The sample printed with 15 % 75 μm MCLP ink showed large cavities inside the gel and absence of lamellar structure. This appearance may be due to the non-uniform distribution of water in the sample and the thin wall layer, which caused considerable water evaporation from the gel network during freeze-drying, resulting in disruption of the gel network structure [36]. The inks with 5 % MCLP were dense, and the gel network structure improved as the particle size increased, aligning with the printing performance results. This may be attributed to the higher fiber content of large particle size as studies have reported that fiber increases the compactness of gel structure leading while contributing to increase the rigidity of the material [21].

3.7. Syneresis of 3D printing food inks

In food inks, syneresis (water spreading) is the undesired leakage of water [13], which results in an unattractive visual appearance (Fig. 5A). Spreading water affects the integrity of printed food structures, resulting in unstable prints that collapse easily. An approach was employed to quantitatively determine the amount of water leaking from the food by measuring the area of Whatman filter paper wet with water on a piece of 3D printed food (Fig. 5B). As the particle size increased, the amount of water leaking from the food products gradually decreased. This finding is consistent with the good water retention found for large granular powders. Water leakage at high concentrations of MCLP was higher than that at low concentrations, which was due to the ability of starch to retain highly viscous water. Therefore, syneresis must be minimized to improve food quality and stability.

3.8. IDDSI test of 3D printing food inks

Dysphagia is common among elderly people, people with mental disabilities, stroke patients, and many postoperative patients, and has a negative impact on their health, well-being, and quality of life [37,38]. Accordingly, the IDDSI developed and published the first international textural standard for special foods for dysphagia (IDDSI International Standard) in 2016 [39], integrating the strengths and weaknesses of national textural standards for special foods. The IDDSI recently launched the IDDSI Textural Framework Version 2.0 [40,41] after more than three years of global practice and promotion.

The IDDSI testing methods were used to determine the IDDSI level classification of the MCLP ink, as shown in Table 1. MCLP ink with a particle size of 75 μm failed the spoon tilt test based on the IDDSI framework, whereas MCLP inks with particle sizes of 131 and 200 μm could be classified as level 5 minced and moist dysphagia diet.

3.9. Correlation between different particle sizes of MCLP and printing properties

Fig. 5C shows the correlation between different particle sizes of the MCLP, gel properties, and printing performance, with red and blue representing positive and negative correlations, respectively, and the correlation coefficient ranging from 1 to -1 . As illustrated in the figure, the MCLP content was negatively correlated with the printing accuracy, which perfectly matches the results in Fig. 3, where a high MCLP content decreased the printing performance. Although the particle size and printing accuracy displayed a positive correlation, the correlation was not strong, which may be attributed to the dependence of the printing performance on both the particle size and the amount of MCLP added to the gel; only a high amount of MCLP led to a significant effect. However, a strong positive correlation was found between chewiness and particle size in MCLP. A similar pattern was observed for gumminess, adhesiveness, and hardness, with hardness showing the highest correlation (0.91). As expected, the WHC and particle size exhibited a strong positive correlation (0.97), which aligns with the results shown in Fig. 1. Moreover, WHC displayed a strong positive correlation with the textural properties: hardness (0.89), chewiness (0.7), and gumminess (0.66) of the MCLP-added corn starch gel; adhesiveness (0.3) exhibited a weak positive correlation. In contrast, syneresis exhibited a strong negative correlation with the following textural properties: hardness (-0.93), chewiness (-0.91), adhesiveness (-0.94), and gumminess (-0.91). Interestingly, syneresis negatively correlated with the particles size (-0.83) of MCLP, where an increase in particles size led to a decrease in syneresis. Printing accuracy and syneresis also displayed a strong negative correlation (-0.75). As expected, G' max strongly correlated with printing accuracy (0.86). The positive correlation displayed between the G' max and the particle size of the MCLP was not strong (0.19). The correlation (0.43) between the printing accuracy and particle size of the MCLP followed a similar trend. Further, G' max and MCLP content showed a strong negative (-0.75) correlation, with an increase in MCLP content leading to a decrease in G' max, resulting in poor printing performance.

4. Conclusions

In this study, several MCLP-corn starch ink mixtures were used for 3D printing. First, the effects of MCLP size and starch addition on the printing performance of the ink were investigated. The addition of starch as a thickening agent was found to increase the apparent viscosity, G' , and G'' , and improve the textural properties of the printed products in a concentration-dependent manner. At high corn starch concentrations, particle size was a major factor in determining textural properties; however, at low starch concentrations, particle size was insignificant in determining textural properties. The printability of the blends was markedly influenced by an increase in the particle size of the incorporated MCLP. This difference was found to be more significant at low starch concentrations. Based on the textural and rheological properties, the current study confirmed that hydrodynamic stability is proportional to particle size. 3D printing inks with 5 % mass fraction of 200 μm MCLP displayed the highest precision, the most ordered microstructure, the most desirable mechanical properties, and good stability. Therefore, suitable material formulations, ratios, and particle sizes are key to successful 3D food printing with the addition of functional ingredients. To enrich and broaden the range of 3D printed food products, future research should focus on nutritional variations and consumer feedback in addition to the study of physical properties.

Funding

This work was supported by the Basic Science Research Program through the National Research Foundation of Korea (NRF), funded by the Ministry of Education, Science, and Technology (grant number NRF-2020R1A2C1014798) and the Research Program for Agricultural Science & Technology Development (grant numbers PJ016130), and the Technology development Program (grant

number S3289574) funded by the Ministry of SME and Startups, Republic of Korea.

Data availability statement

Data has not been deposited in publicly repository but will be made available on request.

CRediT authorship contribution statement

Meiqi Fan: Writing – original draft, Software, Formal analysis, Data curation. **Young-Jin Choi:** Writing – review & editing, Software, Formal analysis. **Nishala Erandi Wedamulla:** Software, Methodology, Investigation, Data curation. **Seok-Hee Kim:** Methodology, Investigation, Data curation. **Sung Mun Bae:** Visualization, Supervision, Conceptualization. **DaEun Yang:** Software, Methodology, Conceptualization. **Hyo Kang:** Software, Methodology, Conceptualization. **Yujiao Tang:** Writing – review & editing, Visualization. **Sang-Ho Moon:** Validation, Supervision, Conceptualization. **Eun-Kyung Kim:** Validation, Supervision, Project administration.

Declaration of competing interest

The authors declare that they have no known competing financial interests or personal relationships that could have appeared to influence the work reported in this paper.

Appendix A. Supplementary data

Supplementary data to this article can be found online at <https://doi.org/10.1016/j.heliyon.2024.e24915>.

References

- [1] D. Venugopal, S. Dhanasekaran, Bitter gourd (*Momordica charantia*) as an emerging therapeutic agent: modulating metabolic regulation and cell signaling cascade, *Stud. Nat. Prod. Chem.* 67 (2020) 221–268, <https://doi.org/10.1016/B978-0-12-819483-6.00007-2>.
- [2] M. Fan, J.I. Lee, Y.B. Ryu, Y.J. Choi, Y. Tang, M. Oh, S.H. Moon, B.K. Lee, E.K. Kim, Comparative analysis of metabolite profiling of *Momordica charantia* leaf and the anti-obesity effect through regulating lipid metabolism, *Int. J. Environ. Res. Publ. Health* 18 (11) (2021) 5584, <https://doi.org/10.3390/ijerph18115584>.
- [3] M.C. Chou, Y.J. Lee, Y.T. Wang, S.Y. Cheng, H.L. Cheng, Cytotoxic and anti-inflammatory triterpenoids in the vines and leaves of *Momordica charantia*, *Int. J. Mol. Sci.* 23 (3) (2022) 1071, <https://doi.org/10.3390/ijms23031071>.
- [4] K.R. Anilakumar, G.P. Kumar, N. Ilaiyaraja, Nutritional, pharmacological and medicinal properties of *Momordica charantia*, *Int. J. Nutr. Food Sci.* 4 (1) (2015) 75–83, <https://doi.org/10.11648/j.jnfs.20150401.21>.
- [5] X. Xing, B. Chitrakar, S. Hati, S. Xie, H. Li, C. Li, Z. Liu, H. Mo, Development of black fungus-based 3D printed foods as dysphagia diet: effect of gums incorporation, *Food Hydrocolloids* 123 (2022) 107173, <https://doi.org/10.1016/j.foodhyd.2021.107173>.
- [6] T. Lorenz, M.M. Iskandar, V. Baeghbali, M.O. Ngadi, S. Kubow, 3D food printing applications related to dysphagia: a narrative review, *Foods* 11 (12) (2022) 1789, <https://doi.org/10.3390/foods11121789>.
- [7] M. Gunjal, P. Rasane, J. Singh, S. Kaur, J. Kaur, Three-dimensional (3D) food printing: methods, processing and nutritional aspects, in: *Food Printing: 3D Printing in Food Industry*, 2022, pp. 65–80, https://doi.org/10.1007/978-981-16-8121-9_5.
- [8] N. Busarac, Z. Jovanovic, Z. Njezić, F. Zivic, N. Grujovic, D. Adamovic, Experimental study and analytical model of shear thinning in 3d bioprinting of gelatin, *Tribology in Industry* 42 (3) (2020) 503–512, <https://doi.org/10.24874/ti.964.09.20.09>.
- [9] J.H. Lee, D.J. Won, H.W. Kim, H.J. Park, Effect of particle size on 3D printing performance of the food-ink system with cellular food materials, *J. Food Eng.* 256 (2019) 1–8, <https://doi.org/10.1016/j.jfoodeng.2019.03.014>.
- [10] K. Abbas, S.K. Khalil, A.S.M. Hussin, Modified starches and their usages in selected food products: a review study, *J. Agric. Sci.* 2 (2) (2010) 90, <https://doi.org/10.5539/jas.v2n2p9>.
- [11] A. Sulaiman, M. Yakubu, Chemical composition of *Momordica charantia* leaves, in: *Proceedings of 105th the IRES International Conference*, 2018, pp. 34–39. Putrajaya, Malaysia. 4-5 March.
- [12] Y C, B.C. Zhang, Y.H. Sun, J.G. Zhang, H.J. Sun, Z.J. Wei, Physicochemical properties and adsorption of cholesterol by okra (*Abelmoschus esculentus*) powder, *Food Funct.* 6 (2015) 3728, <https://doi.org/10.1039/c5fo00600g>.
- [13] A. Pant, A.Y. Lee, R. Karyappa, C.P. Lee, J. An, M. Hashimoto, U. Tan, G. Wong, C.K. Chua, Y. Zhang, 3D food printing of fresh vegetables using food hydrocolloids for dysphagic patients, *Food Hydrocolloids* 114 (2021) 106546, <https://doi.org/10.1016/j.foodhyd.2020.106546>.
- [14] X. Huang, K.H. Liang, Q. Liu, J. Qiu, J. Wang, H. Zhu, Superfine grinding affects physicochemical, thermal and structural properties of *Moringa Oleifera* leaf powders, *Ind. Crop. Prod.* 151 (2020) 112472, <https://doi.org/10.1016/j.indcrop.2020.112472>.
- [15] A. Roth-Nebelsick, D. Uhl, V. Mosbrugger, H. Kerp, Evolution and function of leaf venation architecture: a review, *Ann. Bot.* 87 (5) (2001) 553–566, <https://doi.org/10.1006/anbo.2001.1391>.
- [16] E. Betoret, C.M. Rosell, Effect of particle size on functional properties of Brassica napobrassica leaves powder. Starch interactions and processing impact, *Food Chem. X* 8 (2020) 100106, <https://doi.org/10.1016/j.fochx.2020.100106>.
- [17] S.N. Raghavendra, S.R.R. Swamy, N.K. Rastogi, K.S.M.S. Raghavarao, S. Kumar, R.N. Tharanathan, Grinding characteristics and hydration properties of coconut residue: a source of dietary fiber, *J. Food Eng.* 72 (3) (2006) 281–286, <https://doi.org/10.1016/j.jfoodeng.2004.12.008>.
- [18] H. Gencelepe, F.T. Saricaoglu, M. Anil, B. Agar, S. Turhan, The effect of starch modification and concentration on steady-state and dynamic rheology of meat emulsions, *Food Hydrocolloids* 48 (2015) 135–148, <https://doi.org/10.1016/j.foodhyd.2015.02.002>.
- [19] V.N. Nerella, S. Hempel, V. Mechtcherine, Effects of layer-interface properties on mechanical performance of concrete elements produced by extrusion-based 3D-printing, *Construct. Build. Mater.* 205 (2019) 586–601, <https://doi.org/10.1016/j.conbuildmat.2019.01.235>.
- [20] R. Moreira, F. Chenlo, M.D. Torres, J. Glazer, Rheological properties of gelatinized chestnut starch dispersions: effect of concentration and temperature, *J. Food Eng.* 112 (1–2) (2012) 94–99, <https://doi.org/10.1016/j.jfoodeng.2012.03.021>.

- [21] L. Zheng, J. Liu, R. Liu, Y. Xing, H. Jiang, 3D printing performance of gels from wheat starch, flour and whole meal, *Food Chem.* 356 (2021) 129546, <https://doi.org/10.1016/j.foodchem.2021.129546>.
- [22] Y. Wang, F. Ye, J. Liu, Y. Zhou, L. Lei, G. Zhao, Rheological nature and dropping performance of sweet potato starch dough as influenced by the binder pastes, *Food Hydrocolloids* 85 (2018) 39–50, <https://doi.org/10.1016/j.foodhyd.2018.07.001>.
- [23] A. Gilbert, S.L. Turgeon, Studying stirred yogurt microstructure and its correlation to physical properties: a review, *Food Hydrocolloids* 121 (2021) 106970, <https://doi.org/10.1016/j.foodhyd.2021.106970>.
- [24] Y. Wen, Q.T. Che, H.W. Kim, H.J. Park, Potato starch altered the rheological, printing, and melting properties of 3D-printable fat analogs based on inulin emulsion-filled gels, *Carbohydr. Polym.* 269 (2021) 118285, <https://doi.org/10.1016/j.carbpol.2021.118285>.
- [25] Z. Liu, B. Bhandari, S. Prakash, M. Zhang, Creation of internal structure of mashed potato construct by 3D printing and its textural properties, *Food Res. Int.* 111 (2018) 534–543, <https://doi.org/10.1016/j.foodres.2018.05.075>.
- [26] Z. Liu, M. Zhang, B. Bhandari, C. Yang, Impact of rheological properties of mashed potatoes on 3D printing, *J. Food Eng.* 220 (2018) 76–82, <https://doi.org/10.1016/j.jfoodeng.2017.04.017>.
- [27] F. Sun, Q. Huang, T. Hu, S. Xiong, S. Zhao, Effects and mechanism of modified starches on the gel properties of myofibrillar protein from grass carp, *Int. J. Biol. Macromol.* 64 (2014) 17–24, <https://doi.org/10.1016/j.ijbiomac.2013.11.019>.
- [28] Y. Zhang, G. Li, Y. Wu, Z. Yang, J. Ouyang, Influence of amylose on the pasting and gel texture properties of chestnut starch during thermal processing, *Food Chem.* 294 (2019) 378–383, <https://doi.org/10.1016/j.foodchem.2019.05.070>.
- [29] S. Ji, T. Xu, Y. Liu, H. Li, J. Luo, Y. Zou, Y. Zhong, Y. Li, B. Lu, Investigation of the mechanism of casein protein to enhance 3D printing accuracy of cassava starch gel, *Carbohydr. Polym.* 295 (2022) 119827, <https://doi.org/10.1016/j.carbpol.2022.119827>.
- [30] C. Li, F. Chen, B. Lin, C. Zhang, C. Liu, High content corn starch/Poly (butylene adipate-co-terephthalate) composites with high-performance by physical–chemical dual compatibilization, *Eur. Polym. J.* 159 (2021) 110737, <https://doi.org/10.1016/j.eurpolymj.2021.110737>.
- [31] Y. Zuo, J. Gu, L. Yang, Z. Qiao, H. Tan, Y. Zhang, Synthesis and characterization of maleic anhydride esterified corn starch by the dry method, *Int. J. Biol. Macromol.* 62 (2013) 241–247, <https://doi.org/10.1016/j.ijbiomac.2013.08.032>.
- [32] L. Li, Z. Liu, W. Zhang, B. Xue, Z. Luo, Production and applications of amylose-lipid complexes as resistant starch: recent approaches, *Starch Staerke* 73 (5–6) (2021) 2000249, <https://doi.org/10.1002/star.202000249>.
- [33] P. Guo, J. Yu, S. Wang, S. Wang, L. Copeland, Effects of particle size and water content during cooking on the physicochemical properties and in vitro starch digestibility of milled durum wheat grains, *Food Hydrocolloids* 77 (2018) 445–453, <https://doi.org/10.1016/j.foodhyd.2017.10.021>.
- [34] N.A. Abdulmola, M.W.N. Hember, R.K. Richardson, E.R. Morris, Effect of xanthan on the small-deformation rheology of crosslinked and uncrosslinked waxy maize starch, *Carbohydr. Polym.* 31 (1–2) (1996) 65–78, [https://doi.org/10.1016/S0144-8617\(96\)00065-3](https://doi.org/10.1016/S0144-8617(96)00065-3).
- [35] D. Huc, A. Matignon, P. Barey, M. Desprairies, S. Mauduit, J.M. Sieffermann, C. Michon, Interactions between modified starch and carrageenan during pasting, *Food Hydrocolloids* 36 (2014) 355–361, <https://doi.org/10.1016/j.foodhyd.2013.08.023>.
- [36] C. Tan, S. Pajoumshariati, M. Arshadi, A. Abbaspourrad, A simple route to renewable high internal phase emulsions (HIPEs) strengthened by successive cross-linking and electrostatics of polysaccharides, *Chem. Commun.* 55 (9) (2019) 1225–1228, <https://doi.org/10.1039/C8CC09683J>.
- [37] N. Rommel, S. Hamdy, Oropharyngeal dysphagia: manifestations and diagnosis, *Nat. Rev. Gastroenterol. Hepatol.* 13 (1) (2016) 49–59, <https://doi.org/10.1038/nrgastro.2015.199>.
- [38] T. Warnecke, R. Dziewas, R. Wirth, J.M. Bauer, T. Prell, Dysphagia from a neurogeriatric point of view, *Z. Gerontol. Geriatr.* 52 (4) (2019) 330–335, <https://doi.org/10.1007/s00391-019-01563-x>.
- [39] J.A.Y. Cichero, P. Lam, C.M. Steele, B. Hanson, J. Chen, R.O. Dantas, J. Duivesteyn, J. Kayashita, C. Lecko, J. Murray, M. Pillay, L. Riquelme, S. Stanschus, Development of international terminology and definitions for texture-modified foods and thickened fluids used in dysphagia management: the IDDSI framework, *Dysphagia* 32 (2) (2017) 293–314, <https://doi.org/10.1007/s00455-016-9758-y>.
- [40] D.W. Rule, L. Kelchner, A. Mulkern, S. Couch, N. Silbert, K. Welden, Implementation strategies for the International Dysphagia Diet Standardisation Initiative (IDDSI), part I: quantitative analysis of IDDSI performance among varied participants, *Am. J. Speech Lang. Pathol.* 29 (3) (2020) 1514–1528, https://doi.org/10.1044/2020_AJSLP-19-00012.
- [41] A. Shimizu, K. Maeda, Y. Koyanagi, J. Kayashita, I. Fujishima, N. Mori, The Global Leadership Initiative on Malnutrition—defined malnutrition predicts prognosis in persons with stroke-related dysphagia, *J. Am. Med. Dir. Assoc.* 20 (12) (2019) 1628–1633, <https://doi.org/10.1016/j.jamda.2019.07.008>.